

An Online RFID Localization in the Manufacturing Shopfloor

Andri Ashfahani, Mahardhika Pratama, Edwin Lughofer, Qing Cai and Huang Sheng

Abstract Radio Frequency Identification technology has gained popularity for cheap and easy deployment. In the realm of manufacturing shopfloor, it can be used to track the location of manufacturing objects to achieve better efficiency. The underlying challenge of localization lies in the non-stationary characteristics of manufacturing shopfloor which calls for an adaptive life-long learning strategy in order to arrive at accurate localization results. This paper presents an evolving model based on a novel evolving intelligent system, namely evolving Type-2 Quantum Fuzzy Neural Network (eT2QFNN), which features an interval type-2 quantum fuzzy set with uncertain jump positions. The quantum fuzzy set possesses a graded membership degree which enables better identification of overlaps between classes. The eT2QFNN works fully in the evolving mode where all parameters including the number of rules are automatically adjusted and generated on the fly. The parameter adjustment scenario relies on decoupled extended Kalman filter method. Our numerical study shows that eT2QFNN is able to deliver comparable accuracy compared to state-of-the-art algorithms.

Andri Ashfahani
Nanyang Technological University, Singapore, e-mail: andriash001@e.ntu.edu.sg

Mahardhika Pratama
Nanyang Technological University, Singapore, e-mail: mpratama@ntu.edu.sg

Edwin Lughofer
Johannes Kepler University Linz, Austria, e-mail: edwin.lughofer@jku.at

Qing Cai
Nanyang Technological University, Singapore, e-mail: 506183509@QQ.com

Huang Sheng
Singapore Institute of Manufacturing Technology, Singapore, e-mail: shuang@SIMTech.a-star.edu.sg

1 Introduction

Radio Frequency Identification (RFID) technology has been used to manage objects location in the manufacturing shopfloor. It is more popular than similar technologies for object localization, such as Wireless Sensor Networks (WSN) and WiFi, due to the affordable price and the easy deployment [Ni et al, 2011, Yang et al, 2016].

In the Maintenance, Repair, and Overhaul (MRO) industry, for example, locating the equipments and trolleys manually over the large manufacturing shopfloor area results in time-consuming activities and increases operator work-load. Embracing RFID technology for localization will help companies improve productivity and efficiency in the industry 4.0. Instead of manually locating the tool-trolleys, RFID localization is utilized to monitor the location real-time. Despite much work and progress in RFID localization technology, it is still challenging problems. The key disadvantage of RFID is that it has low quality signal, which is primarily altered by the complexity and severe noises in the manufacturing shopfloors [Chai et al, 2017].

Generally, an RFID localization system comprises of three components, i.e. RFID tag, RFID reader, and the data processing subsystem. The reader aims to identify the tag ID and obtain the received signal strength (RSS) information from tags. An object's location can be estimated by observing the RSS. However, the RSS quality in the real-world is very poor, moreover, it keeps changing over time. As an illustration, although RFID tag is used in the static environment, the RSS keeps changing over time. Moreover, a minor change in the surrounding area can greatly fluctuate the RSS. The major factors causing the phenomena are multipath effect and interference. Therefore, obtaining the accurate location relying on RSS information is a hard task. In several works, those challenges are tackled by employing computational techniques, thus the objects location can be achieved accurately [Ni et al, 2011].

There are several techniques which can be utilized to estimate the object's location. First of all, the distance from an RFID tag to an RFID reader can be calculated via the two-way radar equation for a monostatic transmitter. It can be obtained easily by solving the equation. Another approach, LANDMARC, is proposed for the indoor RFID localization [Ni et al, 2004]. It makes use of K reference tags, and then it evaluates the RSS similarity between reference tags and object tags. A higher weight will be assigned to the reference tags which possess the similar RSS information to the object tags. In the realm of machine learning, support vector regression (SVR) is implemented for the indoor RFID localization [Chai et al, 2017]. It is one-dimensional method and is designed for stationary objects in the small area. Another way to obtain better accuracy is by employing Kalman filter (KF), it has been demonstrated to deal with wavelength ambiguity of the phase measurements [Soltani et al, 2015].

The strategy to estimate the object location via the so-called radar equation is easy to execute. However, the chance to obtain acceptable accuracy is practically impossible due to the severe noises. LANDMARC manage to improve the localization accuracy. Nonetheless, it is difficult to select the reference tag properly in the industrial environments where interference and multipath effect occurred. Improper

selection of reference tags can alter the localization accuracy. Similarly, SVR is also designed to address object localization problem in the small area, it even encounters an over-fitting problem. Meanwhile, integrating KF in some works can improve localization accuracy and it also has low computational cost. KF has better robustness and good statistical properties. However, the requirement to calculate the correlation matrix burdens the computation. In addition, the use of KF is also limited by the nonlinearity and non-stationary condition of the real-world [Chai et al, 2017, Oentaryo et al, 2014]. The data generated from a non-stationary environment can be regarded as the data stream [Pratama, 2017].

Evolving intelligent system (EIS) is an innovation in the field of computational intelligent to deal with data stream [Angelov and Zhou, 2006, Lughofer, 2008]. EIS has an open structure, it implies that it can start the learning processes from scratch or zero rule base. Its rules are automatically formed according to the data stream information. EIS adapts online learning scenario, it conducts the training process in a single-pass mode [Pratama et al, 2016b]. EIS can either adjust the network parameters or generate fuzzy rule without retraining process. Hence, it is capable to deal with the severe noises and the systems dynamics [Lughofer et al, 2015, Pratama et al, 2014b, 2016b]. In several works, the gradient descent (GD) is utilized to adjust the EIS parameters. However, it is vulnerable to noises due to its sensitivity [Oentaryo et al, 2014]. In the premise part, the Gaussian membership function (GMF) is usually employed to capture the input features of EIS. The drawback of GMF is its inadequacy to detect the overlaps between classes. Several works are employed quantum membership function (QMF) to tackle the problem [Chen et al, 2008, Lin and Chen, 2006, Purushothaman and Karayiannis, 1997]. Nevertheless, it is type-1 QMF which is lack of robustness to deal with uncertainties in real-world data streams [Pratama et al, 2016b].

This research proposes an EIS, namely evolving Type-2 Quantum Fuzzy Neural Network (eT2QFNN). The eT2QFNN adopts online learning mechanism, it processes the incoming data one-by-one and the data is discarded after being learned. Thus, eT2QFNN has high efficiency in terms of computational and memory cost. The eT2QFNN is encompassed by two learning policies, i.e. the rule growing mechanism and parameters adjustment. The first mechanism enables eT2QFNN to start the learning process from zero rule base. It can automatically add the rule on demands. Before a new rule is added to the network, it is evaluated by a proposed formulation, namely modified Generalized Type-2 Datum Significance (mGT2DS). The second mechanism performs parameters adjustment whenever a new rule is not formed. It aims to keep the network adapted to the current data stream. This mechanism is accomplished by decoupled extended Kalman filter (DEKF). It is worth noting that the DEKF algorithm performs localized parameter adjustment, i.e. each rule can be adjusted independently [Oentaryo et al, 2014]. In this research, the adjustment is only undertaken on a winning rule, i.e. a rule with the highest contribution. Therefore, DEKF is more efficient than extended Kalman filter (EKF), and yet it still preserves the EKF performance. On the premise part, the interval type-2 QMF (IT2QMF) is proposed to approximate the desired output. It worth noting that it is a universal function approximator which has been demonstrated by several

researchers [Chen et al, 2008, Lin and Chen, 2006, Purushothaman and Karayianis, 1997]. Moreover, it is proficient to form a graded class partition, such that the overlaps between classes can be identified [Chen et al, 2008].

The major contributions of this research are summarized as follows: 1) This research proposes the IT2QMF with uncertain jump position. It is the extended version of QMF. That is, IT2QMF has the interval type-2 capability in terms of incorporating data stream uncertainties. 2) The eT2QFNN is equipped with rule growing mechanism. It can generate its rule automatically in the single-pass learning mode, if a condition is satisfied. The proposed mGT2DS method is employed as the evaluation criterion. 3) The network parameter adjustment relies on DEKF. The mathematical formulation is derived specifically for eT2QFNN architecture. 4) The effectiveness of eT2QFNN has been experimentally validated using real-world RFID localization data.

The remainder of this book chapter is organized as follows. Section II presents the RFID localization system. The proposed type-2 quantum fuzzy membership function and the eT2QFNN network architecture are presented in section III. Section IV presents the learning policies of eT2QFNN and the DEKF for parameter adjustment are discussed. Section V provides empirical studies and comparisons to state-of-the-art algorithms to evaluate the efficacy of eT2QFNN. Finally, section VI concludes this book chapter.

2 RFID Localization System

RFID localization technology has three major components, i.e. RFID tags, RFID readers, and data processing subsystem. There are two types of RFID tags, i.e. the active and passive tag. The active RFID tag is battery-powered and has its own transmitter. It is capable of sending out beacon message, i.e. tag ID and RSS information, actively at specified time window. The transmitted signal can be read up to 300 m radius. In contrast, passive tag does not have independent power source. It exploits the reader power signal, thus it cannot actively send the beacon message in a fixed period of time. The signal can only be read around 1 m radius from the reader, which is very small compared to the manufacturing shopfloor. After that, the transmitted signal is read by the RFID reader. And then it is propagated to the data processing subsystem where the localization algorithm is executed [Ni et al, 2011]. The configuration of RFID localization is illustrated in the Fig. 1.

The RSS information can be utilized to estimate the object location. It can be achieved by solving the two-way radar equation for a monostatic transmitter as per (1). The variables are explained as follows. P_T , G_T , λ , σ , and R are the reader signal power, the antenna gain, carrier wavelength, tag radar cross-section, and the distance between reader and tag, respectively. However, due to the occurrence of multipath effect and interference, the RSS information becomes unreliable and keeps changing over time. Consequently, the satisfying result cannot be obtained [Chai et al, 2017, Ni et al, 2011]. Instead of employing (1) to locate the RFID, this research utilizes

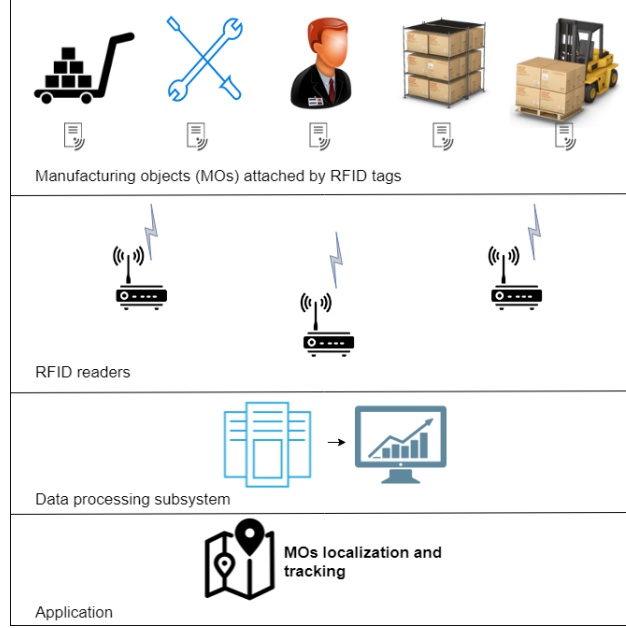


Fig. 1 Architecture of the eT2QFNN

eT2QFNN to process the RSS information to obtain the precise object location.

$$P_R = \frac{G_T^2 \lambda^2 \sigma}{(4\pi)^2 R^4} \text{ (watts)} \quad (1)$$

One of many objectives of this research is to demonstrate the eT2QFNN to deal with the RFID localization problem. The RSS informations of reference tags are utilized to train the network. The reference tags are tags placed at several known and static positions. The eT2QFNN can estimate the new observed tags location according to its RSS. It worth noting that eT2QFNN learning processes are achieved in the evolving mode, it keeps the network parameters and structure adapted to the current data stream. This benefits the network to deal with multipath effect and interference occurred in the manufacturing shopfloor.

Now suppose there are I reference tags which are deployed in M locations, then the RSS measurement vector at n th time-step can be expressed as $X_n = [x_1 \dots x_i \dots x_I]^T$. Afterward, the network outputs for RFID localization problem can be formulated into a multiclass classification problem. As an illustration, if there exist $M = 4$ reference tags deployed in the shopfloor it will indicates that the number of classes is equal to 4.

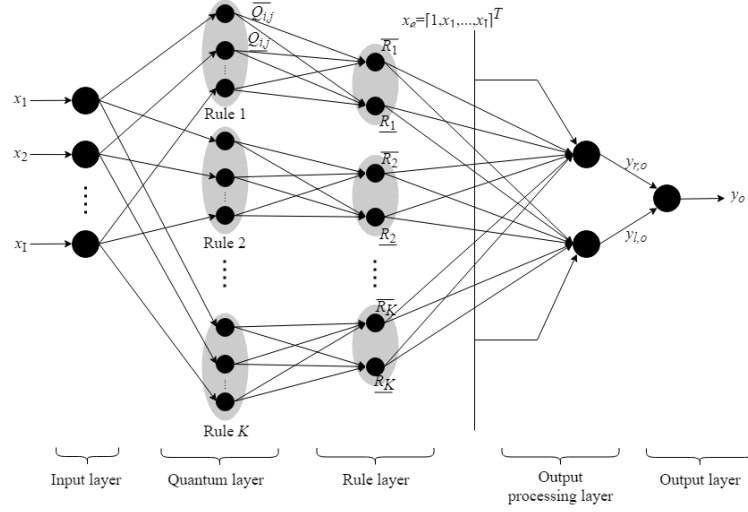


Fig. 2 The RFID localization system

3 eT2QFNN Architecture

This section presents the network architecture of eT2QFNN. The network architecture, as illustrated in the Fig. 2, consists of a five-layer, multi-input-single-output (MISO) network structure. It is systematized into I input features, M outputs nodes and K -term nodes for each input feature. The rule premise is compiled of IT2QMF and is expressed as follows:

$$\mathbf{R}_j : \text{IF } x_1 \text{ is close to } \tilde{Q}_{1j} \text{ and } \dots \text{ and } x_I \text{ is close to } \tilde{Q}_{IK}, \text{ THEN } y_j^o = X_e \tilde{\Omega}_j \quad (2)$$

where x_i and y_j^o are the i th input feature and the regression output of the o th class in the j th rule, respectively. $\tilde{Q}_{ij} = [\bar{Q}_{ij}, \underline{Q}_{ij}]$ denotes the set of upper and lower linguistic term of IT2QMF, X_e is the extended input and $\tilde{\Omega}_j = [\bar{\Omega}_j, \underline{\Omega}_j]$ is the set of upper and lower consequent weight parameters which are defined as $\tilde{\Omega}_j \in \mathfrak{R}^{M \times 2(I+1)}$.

The membership function applied in this study is different from the typical QMF and GMF. The QMF concept is extended into interval type-2 membership function with uncertain jump position. Thus, the network can identify overlaps between classes and capable to deal with the data stream uncertainties. The IT2QMF output of the j th rule for the i th input feature is given in (3)

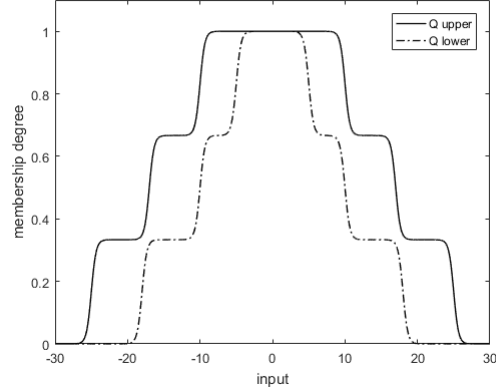


Fig. 3 Interval type-2 quantum membership function with $n_s = 3$

$$\begin{aligned} \tilde{Q}_{ij}(x_{ij}, \beta, m_{ij}, \tilde{\theta}_{ij}) = & \frac{1}{n_s} \sum_{r=1}^{n_s} \left[\left(\frac{1}{1 + \exp(-\beta x_i - m_{ij} + |\tilde{\theta}_{ij}^r|)} \right) U(x_i; -\infty, m_{ij}) \right. \\ & \left. + \left(\frac{\exp(-\beta(x_i - m_{ij} - |\tilde{\theta}_{ij}^r|))}{1 + \exp(-\beta(x_i - m_{ij} - |\tilde{\theta}_{ij}^r|))} \right) U(x_i; m_{ij}, \infty) \right] \quad (3) \end{aligned}$$

where m_{ij} , β , and n_s are mean of i th input feature in j th rule, slope factor, and number of grades, respectively. $\tilde{\theta}_{ij} = [\bar{\theta}_{ij}, \underline{\theta}_{ij}]$ is the set of uncertain jump position, it is defined as $\tilde{\theta}_{ij} \in \mathfrak{R}^{2 \times I \times n_s \times K}$. The upper and lower jump position is expressed as $\bar{\theta}_{ij} = [\bar{\theta}_{1j}^1 \dots \bar{\theta}_{1j}^{n_s}; \dots; \bar{\theta}_{Ij}^1 \dots \bar{\theta}_{Ij}^{n_s}]$ and $\underline{\theta}_{ij} = [\underline{\theta}_{1j}^1 \dots \underline{\theta}_{1j}^{n_s}; \dots; \underline{\theta}_{Ij}^1 \dots \underline{\theta}_{Ij}^{n_s}]$. It is defined that $\bar{\theta}_{ij}^r > \underline{\theta}_{ij}^r$, thus the execution of (3) leads to interval type-2 inference scheme which produces a footprint of uncertainties [Pratama et al, 2016b], it can be clearly seen in the Fig. 3. The eT2QFNN operation in each layer is presented in the following passages.

Input layer

This layer performs no computation. The data stream is directly propagated to the next layer. The input at n th observation is defined by $X_n \in \mathfrak{X}^{1 \times I}$. And the output of the i th node is given as follows:

$$u_i = x_i \quad (4)$$

Quantum layer

This layer performs fuzzification step. IT2QMF is utilized to calculate the membership degrees of X_n in each rule. The number the existing rule is denoted as K . The quantum layer outputs mathematically can be obtained via (5) and (6).

$$\bar{Q}_{ij} = \tilde{Q}_{ij}(x_i, \beta, m_{ij}, \bar{\theta}_{ij}^r) \quad (5)$$

$$\underline{Q}_{ij} = \tilde{Q}_{ij}(x_i, \beta, m_{ij}, \underline{\theta}_{ij}^r) \quad (6)$$

Rule layer

This layer functions to combine the membership degree of j th rule denoted as $\tilde{R}_j = [\bar{R}_j, \underline{R}_j]$, which is known as spatial firing strength. This can be achieved by employing product T-norm of IT2QMF, as per (7) and (8). The set of upper and lower firing strengths are expressed as $\bar{R} = [\bar{R}_1 \dots \bar{R}_K]$ and $\underline{R} = [\underline{R}_1 \dots \underline{R}_K]$, respectively.

$$\bar{R}_j = \prod_{i=1}^I \bar{Q}_{ij} \quad (7)$$

$$\underline{R}_j = \prod_{i=1}^I \underline{Q}_{ij} \quad (8)$$

Output processing layer

The calculation of the two endpoints output, i.e. $y_{l,o}$ and $y_{r,o}$, is conducted here. These variables represent the lower and upper crisp output of the o th class, respectively. The design factor $[q_l, q_r]$ are employed to convert the interval type-2 variable to type-1 variable, this is known as the type reduction procedure. This requires less iterative steps compare to the Karnik Mendel (KM) type reduction procedure [Pratama et al, 2016a]. The design factor will govern the proportion of upper and lower IT2QMF and it is defined such that $q_l < q_r$. The design factor is adjusted using DEKF, thus the proportion of upper and lower outputs $[y_l, y_r]$ keeps adapting to the data streams uncertainties. The lower and upper outputs are given as:

$$y_{l,o} = \frac{(1-q_{l,o}) \sum_{j=1}^K \underline{R}_j \underline{\Omega}_{jo} x_e^T + q_{l,o} \sum_{j=1}^K \bar{R}_j \underline{\Omega}_{jo} x_e^T}{\sum_{j=1}^K (\bar{R}_j + \underline{R}_j)} \quad (9)$$

$$y_{r,o} = \frac{(1-q_{r,o}) \sum_{j=1}^K \underline{R}_j \bar{\Omega}_{jo} x_e^T + q_{r,o} \sum_{j=1}^K \bar{R}_j \bar{\Omega}_{jo} x_e^T}{\sum_{j=1}^K (\bar{R}_j + \underline{R}_j)} \quad (10)$$

where $q_l = [q_{l,1}, \dots, q_{l,M}]$, $q_r = [q_{r,1}, \dots, q_{r,M}]$ are the design factors of all classes, while $\bar{\Omega}_{jo} = [\bar{w}_{ij}^o, \dots, \bar{w}_{(I+1)j}^o]$, and $\underline{\Omega}_{jo} = [w_{ij}^o, \dots, w_{(I+1)j}^o]$ express the upper and lower consequent weight parameters of the j th rule for the o th class. In addition, $x_e \in \Re^{(I+1) \times 1}$ is the extended input vector. For example, X_n has I input features $[x_1, \dots, x_I]$, then the extended input vector is $X_e = [1, x_1, \dots, x_I]$. The entry 1 is included to incorporate the intercept of the rule consequent and to prevent the untypical gradient [Pratama et al, 2016b].

Output layer

The crisp network output of the o th class is the sum of $y_{l,o}$ and $y_{r,o}$ as per (11). Furthermore, if the network structure of eT2QFNN is utilized to deal with multiclass classification, the multi-model (MM) classifier can be employed to obtain the final

Algorithm 1 Learning policy of eT2QFNN

Define: input-output pair $X_n = [x_1, \dots, x_J]^T$, $T_n = [t_1, \dots, t_M]^T$, n_s , and η

\\Phase 1: Rule Growing Mechanism

If $K = 0$ **then**
 Initiate the first rule via (26), (29), and (30)
else
 Approximate the existing IT2QMF via (18)
 Initiate a hypothetical rule R_{K+1} via (26), (27), and (31)
for $j = 1$ **to** $K + 1$
 Calculate the statistical contribution E_j via (20)
end for
If $E_{K+1} \geq \rho \sum_{j=1}^K E_j$ **then**
 $K = K + 1$
end if
end if

\\Phase 2: Parameter Adjustment using DEKF

If $K(n) = K(n-1)$ **then**
 Calculate the spatial firing strength via (7) and (8)
 Determine the winning rule j_w via (34)
 Do DEKF adjustment mechanism on rule R_{j_w} via (37) and (39)
 Update covariance matrix of the winning rule via (38)
else
 Initialize the new rule consequents weight $\tilde{\Omega}_{K+1}$ and covariance matrix and as (31) and (32)
for $j = 1$ **to** $K - 1$ **do**
 $P_j(n) = P_j(n-1) \left(\frac{K^2+1}{K^2} \right)$
end for
end if

classification decision. The MM classifier splits the multiclass classification problem into K binary sub-problems, then K MISO eT2QFNN is built accordingly. The final class decision is the index number o of the highest output, as per (12).

$$y_o = y_{l,o} + y_{r,o} \quad (11)$$

$$y = \arg \max_{o=1, \dots, M} y_o \quad (12)$$

4 eT2QFNN Learning Policy

The online learning mechanism of eT2QFNN consists of two scenarios, i.e. the rule growing and the parameter adjustment which is executed in every iteration. The eT2QFNN starts its learning process with an empty rule base and keeps updating its parameters and network structure as the observation data comes in. The proposed learning scenario is presented in the Algorithm 1, while subsections 4.1 and 4.2 further explain the learning scenarios.

4.1 Rule growing mechanism

The eT2QFNN is capable of automatically evolving its fuzzy rule on demands using the proposed mGT2DQ method. First of all, it is achieved by forming a hypothetical rule from a newly seen sample. The initialization of hypothetical rule parameters is presented in the sub-subsection 4.2.1. Before it is added to the network, it is required to evaluate its significance. The significance of the j th rule is defined as an L^2 -norm of $E_{sig}(j)$ weighted by the input density function $p(x)$ as follows [Huang et al, 2005]:

$$E_{sig}(j) = \|\omega_j\| \left(\int_{\mathcal{R}^I} \exp(-2\|X - m_j\|^2/\sigma_j^2) p(X) dX \right)^{1/2} \quad (13)$$

From the (13), it is obvious that the input density $p(X)$ greatly contributes to $E_{sig}(j)$. In practical, it is hard to be calculate a priori because the data distribution is unknown. Huang et al [2003] and Huang et al [2004] calculated (13) analytically with the assumption of $p(X)$ being uniformly distributed. However, Zhang et al [2004] demonstrated that it leads to performance degradation for complex $p(X)$. To overcome this problem, Bortman and Aladjem [2009] proposed Gaussian mixture model (GMM) to approximate the complicated data stream density. The mathematical formulation of GMM is given as:

$$\hat{p}(X) = \sum_{h=1}^H \alpha_h \mathcal{N}(X; v_h, \Sigma_h) \quad (14)$$

$$\mathcal{N}(X; v_h, \Sigma_h) = \exp(-(X - v_h)^T \Sigma_h^{-1} (X - v_h)) \quad (15)$$

where $\mathcal{N}(X; v_h, \Sigma_h)$ is the Gaussian function of variable X as per (15), with the mean vector $v_h \in \mathcal{R}^I$, variance matrix $\Sigma_h \in \mathcal{R}^{I \times I}$, H denotes the number of mixture model, and α_h represent the mixing coefficients ($\sum_{h=1}^H \alpha_h = 1; \alpha_h > 0 \forall h$).

In the next step, the estimated significance of j th rule $\hat{E}_{sig}(j)$ is calculated. Vuković and Miljković [2013] derived the mathematical formulation to obtain $\hat{E}_{sig}(j)$ by substituting (14) to (13) and then solving the closed form analytical solution, it yields to the following result:

$$\hat{E}_{sig}(j) = \|\omega_j\| (\pi^{I/2} \det(\Sigma_j)^{1/2} N_j A^T)^{1/2} \quad (16)$$

where $A = [\alpha_1, \dots, \alpha_H]$ is the vector of GMM mixing coefficients, Σ_j denotes as the positive definite weighting matrix which is expressed as $\Sigma_j = \text{diag}(\sigma_{1,j}^2, \dots, \sigma_{I,j}^2)$, and N_j is given as:

$$N_j = [\mathcal{N}(m_j - v_1; 0, \Sigma_j/2 + \Sigma_1), \mathcal{N}(m_j - v_2; 0, \Sigma_j/2 + \Sigma_2), \dots, \mathcal{N}(m_j - v_H; 0, \Sigma_j/2 + \Sigma_H)] \quad (17)$$

where m_j is the mean vector of j th rule defined as $m_j = [m_{1,j}, \dots, m_{I,j}]$. And the GMM parameters v_h , Σ_h , and A can be calculated by exploiting $N_{history}$ pre-recorded

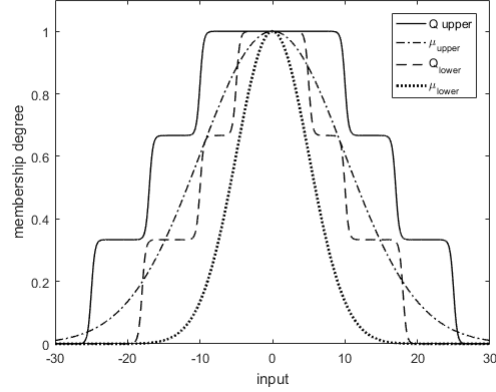


Fig. 4 The comparison result of IT2QMF and IT2GMF

data. This technique is feasible and easy to implement because the pre-recorded input data is most likely to be stored especially in the era of data stream. The number of pre-recorded data is somewhat smaller than the training data, it is denoted as $N_{history} \ll N$. It is not problem-specific and it can be set to a fixed value [Pratama, 2017]. In this research, it is set as 50 for simplicity.

The method (16) could not, however, be applied directly to estimate the eT2QFNN rule significance, because eT2QFNN utilizes IT2QMF instead of Gaussian membership function (GMF). The key idea to overcome this problem is by approximating IT2QMF using interval type-2 Gaussian Membership Function (IT2GMF). The mathematical formulation of this approach can be written as follows:

$$\tilde{Q}_{i,j}(x_i, \beta, m_{i,j}, \tilde{\theta}_{i,j}) \approx \tilde{\mu}_{i,j} = \exp\left(-\frac{(x_i - m_{i,j})^2}{\tilde{\sigma}_{i,j}}\right) \quad (18)$$

$$\tilde{\sigma}_{i,j} = [\underline{\sigma}_{i,j}, \bar{\sigma}_{i,j}]$$

$$\underline{\sigma}_{i,j} = \min \underline{\theta}_{i,j}; \quad \bar{\sigma}_{i,j} = \min \bar{\theta}_{i,j} \quad (19)$$

The mean of IT2GMF is defined to equal the mean of IT2QMF, i.e. m_{ij} . And the width of upper and lower IT2GMF are obtained by taking the minimum value of $\tilde{\theta}_{ij}$ as per (19). By selecting these criteria, the whole area of IT2GMF will be located inside the area of IT2QMF. As illustrated in the Fig. 4, both upper and lower area of IT2GMF covers the appropriate area of IT2QMF. Therefore, this approach can provide a good approximation of IT2QMF.

Afterward, the proposed method to estimate eT2QFNN rule significance can be derived by executing (16) with the design factor as per (20). In (21) and (22), $\bar{\underline{\Omega}}_j = [\bar{\underline{\Omega}}_{j,1}, \dots, \bar{\underline{\Omega}}_{j,M}]^T$ and $\underline{\underline{\Omega}}_j = [\underline{\underline{\Omega}}_{j,1}, \dots, \underline{\underline{\Omega}}_{j,M}]^T$ are denoted as the upper and lower consequent weight parameters of all classes, respectively. The variance matrices $\bar{\Sigma}_j$ and $\underline{\Sigma}_j$ are formed of $\bar{\sigma}_{i,j}$ and $\underline{\sigma}_{i,j}$ as per (24), while \bar{N}_j and \underline{N}_j are given in (25). The hypothetical rule will be added to the network as a new rule \mathbf{R}_{K+1} if it posses

statistical contribution over existing rules. The mathematical formulation of rule growing criterion is given in (23), where the constant $\rho \in (0, 1]$ is defined as the vigilance parameter and in this research it is fixed at 0.65 for simplicity.

$$\hat{E}_j = |\hat{E}_{j,l}| + |\hat{E}_{j,r}| \quad (20)$$

$$\begin{aligned} \hat{E}_{j,l} = & \|q_l\| \cdot \|\bar{\Omega}_j\| \cdot (\pi^{I/2} \det(\bar{\Sigma}_j)^{1/2} \bar{N}_j A^T)^{1/2} \\ & + (1 - \|q_l\|) \cdot \|\underline{\Omega}_j\| \cdot (\pi^{I/2} \det(\underline{\Sigma}_j)^{1/2} \underline{N}_j A^T)^{1/2} \end{aligned} \quad (21)$$

$$\begin{aligned} \hat{E}_{j,r} = & \|q_r\| \cdot \|\bar{\Omega}_j\| \cdot (\pi^{I/2} \det(\bar{\Sigma}_j)^{1/2} \bar{N}_j A^T)^{1/2} \\ & + (1 - \|q_r\|) \cdot \|\underline{\Omega}_j\| \cdot (\pi^{I/2} \det(\underline{\Sigma}_j)^{1/2} \underline{N}_j A^T)^{1/2} \end{aligned} \quad (22)$$

$$E_{K+1} \geq \rho \sum_{j=1}^K E_j \quad (23)$$

$$\bar{\Sigma}_j = \text{diag}(\bar{\sigma}_{1,j}^2, \dots, \bar{\sigma}_{I,j}^2), \quad \underline{\Sigma}_j = \text{diag}(\underline{\sigma}_{1,j}^2, \dots, \underline{\sigma}_{I,j}^2) \quad (24)$$

$$\begin{aligned} \bar{N}_j = & [\mathcal{N}(m_j - v_1; 0, \bar{\Sigma}_j/2 + \Sigma_1), \mathcal{N}(m_j - v_2; 0, \bar{\Sigma}_j/2 + \Sigma_2), \dots \\ & \dots, \mathcal{N}(m_j - v_H; 0, \bar{\Sigma}_j/2 + \Sigma_H)], \\ \underline{N}_j = & [\mathcal{N}(m_j - v_1; 0, \underline{\Sigma}_j/2 + \Sigma_1), \mathcal{N}(m_j - v_2; 0, \underline{\Sigma}_j/2 + \Sigma_2), \dots \\ & \dots, \mathcal{N}(m_j - v_H; 0, \underline{\Sigma}_j/2 + \Sigma_H)] \end{aligned} \quad (25)$$

4.2 Parameter adjustment

This phase comprises of two alternative strategies. The first strategy is carried out to form a hypothetical rule. It will be added into the network structure if the condition in (23) is satisfied. This strategy is called the fuzzy rule initialization. And the second mechanism is executed whenever (23) is not satisfied. It is aimed to adjust the network parameters according to the current data stream. This is called the winning rule update. These strategies are elaborated in the following sub-subsections.

4.2.1 Fuzzy rule initialization

The rule growing mechanism first of all is conducted by forming a hypothetical rule according to the current data stream. The data at n th time-step X_n is assigned as the new mean of IT2QMF, as per (26). And then, the new jump position is achieved via distance-based formulation inspired by [Lin and Chen, 2006], as per (27). In this research, however, it is modified such that the new distance $\tilde{\sigma}_{i,K+1}$ is obtained utilizing the mixed mean of GMM \hat{v} , as per (28). Thanks to the GMM features which is able to approximate the mean and variance of very complex input. For this reason, instead of using $\tilde{\sigma}_{i,K+1}$ to calculate the jump position of the first rule in (29), the eT2QFNN utilizes the diagonal entries of the mixed variance matrix, as per (30).

The constant δ_1 is introduced to create the footprint of uncertainty. In this study, it is set $\delta_1 = 0.7$ for simplicity.

In the next stage, the consequent weight parameters of hypothetical rule are determined. It is equal to the consequent weight of the winning rule as per (31). The key idea behind this strategy is to acquire the knowledge of winning rule in terms of representing the current data stream [Oentaryo et al, 2014]. The way to select the winning rule is presented in sub-subsection (4.2.2). Finally, if the hypothetical rule passes the evaluation criterion in (23), it is added as the new rule (\mathbf{R}_{K+1}) and its covariance matrix is initialized via (32).

In contrast, a consideration is required to adjust the covariance matrices of other rules, because the new rule formation corrupts those matrices. This phenomenon has been investigated in SPLAFIS [Oentaryo et al, 2014], the research revealed that those matrices need to be readjusted. The proper readjustment technique is achieved by multiplication of those matrices and $\left(\frac{K^2+1}{K^2}\right)$ as per (33). This strategy is signified to take into account the contribution that a new rule would have if it existed from the first iteration. It, therefore, will decrease the corruption effect [Oentaryo et al, 2014].

$$m_{K+1} = X_n \quad (26)$$

$$\bar{\theta}_{i,K+1}^r = \frac{1}{((n_s + 1)/2)} \cdot r \cdot \bar{\sigma}_{i,K+1},$$

$$\underline{\theta}_{i,K+1}^r = \frac{1}{((n_s + 1)/2)} \cdot r \cdot \underline{\sigma}_{i,K+1} \quad (27)$$

$$\bar{\sigma}_{i,K+1} = |X_n - \hat{v}|, \quad \underline{\sigma}_{i,K+1} = \delta_1 \cdot \bar{\sigma}_{i,K+1} \quad (28)$$

$$\hat{v} = \sum_{h=1}^H \alpha_h \cdot v_h$$

$$\bar{\theta}_{i,1}^r = \frac{1}{((n_s + 1)/2)} \cdot r \cdot \bar{\sigma}_{i,1},$$

$$\underline{\theta}_{i,1}^r = \frac{1}{((n_s + 1)/2)} \cdot r \cdot \underline{\sigma}_{i,1} \quad (29)$$

$$\bar{\sigma}_{i,1} = \hat{\sigma}_i, \quad \underline{\sigma}_{i,1} = \delta_1 \cdot \bar{\sigma}_{i,1} \quad (30)$$

$$\hat{\Sigma} = \sum_{h=1}^H \Sigma_h \cdot v_h, \quad \hat{\Sigma} = \text{diag}(\hat{\sigma}_1^2, \dots, \hat{\sigma}_J^2)$$

$$\tilde{\Omega}_{K+1} = \tilde{\Omega}_{j_w} \quad (31)$$

$$P_{K+1}(n) = I_{Z \times Z} \quad (32)$$

$$P_j(n) = \left(\frac{K^2+1}{K^2}\right) P_j(n-1) \quad (33)$$

4.2.2 Winning rule update

The hypothetical rule would not be added to the network structure if it failed the evaluation in (23). To maintain the eT2QFNN performance, the network parameters is required to be adjusted according to the information provided by the current data stream. In this research, the adjustment is only undertaken on the winning rule which is defined as a rule having the highest average of the spatial firing strength. The mathematical formulation is given in (34). It worth noting that spatial firing strength represents the degree to which the rule antecedent part is satisfied. The rule having higher firing strength possesses higher correlation to the current data stream [Pratama et al, 2014b], therefore it deserves to be adjusted.

$$j_w = \arg \max_j \tilde{R}_j \quad (34)$$

$$\tilde{R}_j = \frac{\bar{R}_j + R_j}{2} \quad (35)$$

Previously, DEKF is employed to adjust the winning rule parameters of type-1 fuzzy neural network. It is capable of maintaining local learning property of EIS because it can adjust parameters locally [Oentaryo et al, 2014]. In this research, DEKF is utilized to update the winning rule parameters of eT2QFNN. The local parameters are classified by rule, i.e. the parameters in the same rule are grouped together. This leads to the formation of block-diagonal covariance matrix $\tilde{P}(n)$ as per (36). There is only one block covariance matrix updated in each time-step, i.e. $P_{j_w}(n)$. The localized adjustment property of DEKF enhances the algorithm efficiency in terms of computational complexity and memory requirements, moreover it still maintains the same robustness as the EKF [Puskorius and Feldkamp, 1994].

$$\tilde{P}(n) = \begin{bmatrix} P_1(n) & \dots & 0 & \dots & 0 \\ \vdots & \ddots & & & \vdots \\ 0 & & P_j(n) & & 0 \\ \vdots & & & \ddots & \vdots \\ 0 & \dots & 0 & \dots & P_K(n) \end{bmatrix} \quad (36)$$

The mathematical formulations of DEKF algorithm are given in (37)-(39). The designation of each parameter in the equation is as follows. $G_{j_w}(n)$ and $P_{j_w}(n)$ are the Kalman gain matrix and covariance matrix, respectively. The covariance matrix represents the interaction between each pair of the parameters in the network. $\vec{\theta}_{j_w}(n)$ is the parameter vector of \mathbf{R}_{j_w} at n th iteration, it consists of all the network parameters which is about to be adjusted. It is expressed as $\vec{\theta}_{j_w}(n) = [\underline{\Omega}_{j_w}^T, \bar{\Omega}_{j_w}^T, q_l^T, q_r^T, m_{j_w}^T, \underline{\theta}_{j_w}^T, \bar{\theta}_{j_w}^T]^T$, which is respectively given in (40)-(46). The length of $\vec{\theta}_{j_w}(n)$ is equal to $Z = 2 \times M \times (2 + I) + I \times (2 \times n_s + 1)$. The Jacobian matrix $H_{k_w}(n)$, presented in (47), contains the output gradient with respect to the network parameters, and it is arranged into Z -by- M matrix. The gradient vectors

are specified in (48) and is calculated using (49)-(52). The output and target vectors are defined as $y(n) = [y_1(n) \dots y_M(n)]$ and $t(n) = [t_1(n) \dots t_M(n)]$. It is utilized to calculate the error vector in (39). The last parameters, η , is a learning rate parameter [Puskorius and Feldkamp, 1994]. This completes the second strategy to maintain the network adapted to the current data stream.

$$G_{j_w}(n) = P_{j_w}(n-1)H_{j_w}(n)[\eta I_{M \times M} + H_{k_w}^T(n)P_{j_w}(n-1)H_{j_w}(n)]^{-1} \quad (37)$$

$$P_{j_w}(n) = [I_{Z \times Z} - G_{j_w}(n)H_{j_w}^T(n)]P_{j_w}(n-1) \quad (38)$$

$$\vec{\theta}_{j_w}(n) = \vec{\theta}_{j_w}(n-1) + G_{j_w}(n)[t(n) - y(n)] \quad (39)$$

$$\underline{\Omega}_{j_w} = [\underline{\Omega}_{1,j_w}^1, \dots, \underline{\Omega}_{I+1,j_w}^1, \dots, \underline{\Omega}_{1,j_w}^M, \dots, \underline{\Omega}_{I+1,j_w}^M]^T \quad (40)$$

$$\overline{\Omega}_{j_w} = [\overline{\Omega}_{1,j_w}^1, \dots, \overline{\Omega}_{I+1,j_w}^1, \dots, \overline{\Omega}_{1,j_w}^M, \dots, \overline{\Omega}_{I+1,j_w}^M]^T \quad (41)$$

$$q_l = [q_{l,1}, \dots, q_{l,M}]^T \quad (42)$$

$$q_r = [q_{r,1}, \dots, q_{r,M}]^T \quad (43)$$

$$m_{j_w} = [m_{1,j_w}, \dots, m_{I,j_w}]^T \quad (44)$$

$$\underline{\theta}_{j_w} = [\underline{\theta}_{1,j_w}^1, \dots, \underline{\theta}_{I,j_w}^1, \dots, \underline{\theta}_{1,j_w}^{n_s}, \dots, \underline{\theta}_{I,j_w}^{n_s}]^T \quad (45)$$

$$\overline{\theta}_{j_w} = [\overline{\theta}_{1,j_w}^1, \dots, \overline{\theta}_{I,j_w}^1, \dots, \overline{\theta}_{1,j_w}^{n_s}, \dots, \overline{\theta}_{I,j_w}^{n_s}]^T \quad (46)$$

$$H_{j_w}(n) = \begin{bmatrix} \frac{\partial y_1}{\partial \underline{\Omega}_{j_w,1}} & \dots & 0 & \dots & 0 \\ 0 & \dots & \frac{\partial y_o}{\partial \underline{\Omega}_{j_w,o}} & \dots & 0 \\ 0 & \dots & 0 & \dots & \frac{\partial y_M}{\partial \underline{\Omega}_{j_w,M}} \\ \frac{\partial y_1}{\partial \overline{\Omega}_{j_w,1}} & \dots & 0 & \dots & 0 \\ 0 & \dots & \frac{\partial y_o}{\partial \overline{\Omega}_{j_w,o}} & \dots & 0 \\ 0 & \dots & 0 & \dots & \frac{\partial y_M}{\partial \overline{\Omega}_{j_w,M}} \\ \frac{\partial y_1}{\partial q_{l,1}} & \dots & 0 & \dots & 0 \\ 0 & \dots & \frac{\partial y_o}{\partial q_{l,o}} & \dots & 0 \\ 0 & \dots & 0 & \dots & \frac{\partial y_M}{\partial q_{l,M}} \\ \frac{\partial y_1}{\partial q_{r,1}} & \dots & 0 & \dots & 0 \\ 0 & \dots & \frac{\partial y_o}{\partial q_{r,o}} & \dots & 0 \\ 0 & \dots & 0 & \dots & \frac{\partial y_M}{\partial q_{r,M}} \\ \frac{\partial y_1}{\partial m_{j_w,1}} & \dots & \frac{\partial y_o}{\partial m_{j_w,o}} & \dots & \frac{\partial y_M}{\partial m_{j_w,M}} \\ \frac{\partial y_1}{\partial \underline{\theta}_{j_w,1}} & \dots & \frac{\partial y_o}{\partial \underline{\theta}_{j_w,o}} & \dots & \frac{\partial y_M}{\partial \underline{\theta}_{j_w,M}} \\ \frac{\partial y_1}{\partial \overline{\theta}_{j_w,1}} & \dots & \frac{\partial y_o}{\partial \overline{\theta}_{j_w,o}} & \dots & \frac{\partial y_M}{\partial \overline{\theta}_{j_w,M}} \end{bmatrix} \quad (47)$$

$$\begin{aligned}
\frac{\partial y_o}{\partial \underline{\Omega}_{j_w,o}} &= \left[\frac{\partial y_o}{\partial \underline{w}_{1,j_w}^o}, \dots, \frac{\partial y_o}{\partial \underline{w}_{I+1,j_w}^o} \right]^T, & \frac{\partial y_o}{\partial \bar{\Omega}_{j_w,o}} &= \left[\frac{\partial y_o}{\partial \bar{w}_{1,j_w}^o}, \dots, \frac{\partial y_o}{\partial \bar{w}_{I+1,j_w}^o} \right]^T, \\
\frac{\partial y_o}{\partial m_{j_w,o}} &= \left[\frac{\partial y_o}{\partial m_{1,j_w}^o}, \dots, \frac{\partial y_o}{\partial m_{I,j_w}^o} \right]^T, \\
\frac{\partial y_o}{\partial \underline{\theta}_{j_w,o}} &= \left[\frac{\partial y_o}{\partial \underline{\theta}_{1,j_w,o}^1}, \dots, \frac{\partial y_o}{\partial \underline{\theta}_{I,j_w,o}^1}, \dots, \frac{\partial y_o}{\partial \underline{\theta}_{1,j_w,o}^{n_s}}, \dots, \frac{\partial y_o}{\partial \underline{\theta}_{I,j_w,o}^{n_s}} \right]^T, \\
\frac{\partial y_o}{\partial \bar{\theta}_{j_w,o}} &= \left[\frac{\partial y_o}{\partial \bar{\theta}_{1,j_w,o}^1}, \dots, \frac{\partial y_o}{\partial \bar{\theta}_{I,j_w,o}^1}, \dots, \frac{\partial y_o}{\partial \bar{\theta}_{1,j_w,o}^{n_s}}, \dots, \frac{\partial y_o}{\partial \bar{\theta}_{I,j_w,o}^{n_s}} \right]^T
\end{aligned} \tag{48}$$

$$\begin{aligned}
\frac{\partial y_o}{\partial \underline{w}_{1,j_w}^o} &= \left[\frac{(1 - q_{l,o})\underline{R}_{j_w} + q_{l,o}\bar{R}_{j_w}}{\sum_{j=1}^K (\underline{R}_{j_w} + \bar{R}_{j_w})} \right] x_{e,i}(n), \\
\frac{y_o}{\partial \bar{w}_{1,j_w}^o} &= \left[\frac{(1 - q_{r,o})\underline{R}_{j_w} + q_{r,o}\bar{R}_{j_w}}{\sum_{j=1}^K (\underline{R}_{j_w} + \bar{R}_{j_w})} \right] x_{e,i}(n)
\end{aligned} \tag{49}$$

$$\begin{aligned}
\frac{\partial y_o}{\partial q_{l,o}} &= \left[\frac{-\sum_{j=1}^K \underline{R}_j \underline{\Omega}_o + \sum_{j=1}^K \bar{R}_j \underline{\Omega}_o}{\sum_{j=1}^K (\underline{R}_{j_w} + \bar{R}_{j_w})} \right] X_e(n), \\
\frac{\partial y_o}{\partial q_{r,o}} &= \left[\frac{-\sum_{j=1}^K \underline{R}_j \bar{\Omega}_o + \sum_{j=1}^K \bar{R}_j \bar{\Omega}_o}{\sum_{j=1}^K (\underline{R}_{j_w} + \bar{R}_{j_w})} \right] X_e(n)
\end{aligned} \tag{50}$$

$$\begin{aligned}
\frac{\partial y_o}{\partial m_{i,j_w}} &= \frac{\partial y_o}{\partial y_{l,o}} \left[\frac{\partial y_{l,o}}{\partial \underline{R}_{j_w}} \frac{\partial \underline{R}_{j_w}}{\partial m_{i,j_w}} + \frac{\partial y_{l,o}}{\partial \bar{R}_{j_w}} \frac{\partial \bar{R}_{j_w}}{\partial m_{i,j_w}} \right] \\
&+ \frac{\partial y_o}{\partial y_{r,o}} \left[\frac{\partial y_{r,o}}{\partial \underline{R}_{j_w}} \frac{\partial \underline{R}_{j_w}}{\partial m_{i,j_w}} + \frac{\partial y_{r,o}}{\partial \bar{R}_{j_w}} \frac{\partial \bar{R}_{j_w}}{\partial m_{i,j_w}} \right]
\end{aligned} \tag{51}$$

$$\begin{aligned}
\frac{\partial y_o}{\partial \underline{\theta}_{i,j_w}^r} &= \frac{\partial y_o}{\partial y_{l,o}} \frac{\partial y_{l,o}}{\partial \underline{R}_{j_w}} \frac{\partial \underline{R}_{j_w}}{\partial \underline{\theta}_{i,j_w}^r} + \frac{\partial y_o}{\partial y_{r,o}} \frac{\partial y_{r,o}}{\partial \underline{R}_{j_w}} \frac{\partial \underline{R}_{j_w}}{\partial \underline{\theta}_{i,j_w}^r}, \\
\frac{\partial y_o}{\partial \bar{\theta}_{i,j_w}^r} &= \frac{\partial y_o}{\partial y_{l,o}} \frac{\partial y_{l,o}}{\partial \bar{R}_{j_w}} \frac{\partial \bar{R}_{j_w}}{\partial \bar{\theta}_{i,j_w}^r} + \frac{\partial y_o}{\partial y_{r,o}} \frac{\partial y_{r,o}}{\partial \bar{R}_{j_w}} \frac{\partial \bar{R}_{j_w}}{\partial \bar{\theta}_{i,j_w}^r}
\end{aligned} \tag{52}$$

$$\begin{aligned}
\frac{\partial y_o}{\partial y_{l,o}} &= \frac{\partial y_o}{\partial y_{l,o}} = 1 \\
\frac{\partial y_{l,o}}{\partial \underline{R}_{j_w}} &= \frac{(1 - q_{l,o})\underline{\Omega}_{j_w,o}X_e(n)}{\sum_{j=1}^K(\underline{R}_j + \bar{R}_j)} - \frac{(1 - q_{l,o})\underline{R}\underline{\Omega}_mX_e(n) + q_{l,o}\bar{R}\underline{\Omega}_mX_e(n)}{(\sum_{j=1}^K(\underline{R}_j + \bar{R}_j))^2} \\
\frac{\partial y_{l,o}}{\partial \bar{R}_{j_w}} &= \frac{q_{l,o}\underline{\Omega}_{j_w,o}X_e(n)}{\sum_{j=1}^K(\underline{R}_j + \bar{R}_j)} - \frac{(1 - q_{l,o})\underline{R}\underline{\Omega}_mX_e(n) + q_{l,o}\bar{R}\underline{\Omega}_mX_e(n)}{(\sum_{j=1}^K(\underline{R}_j + \bar{R}_j))^2} \\
\frac{\partial y_{r,o}}{\partial \underline{R}_{j_w}} &= \frac{(1 - q_{r,o})\underline{\Omega}_{j_w,o}X_e(n)}{\sum_{j=1}^K(\underline{R}_j + \bar{R}_j)} - \frac{(1 - q_{r,o})\underline{R}\underline{\Omega}_mX_e(n) + q_{r,o}\bar{R}\underline{\Omega}_mX_e(n)}{(\sum_{j=1}^K(\underline{R}_j + \bar{R}_j))^2} \\
\frac{\partial y_{r,o}}{\partial \bar{R}_{j_w}} &= \frac{q_{r,o}\bar{\Omega}_{j_w,o}X_e(n)}{\sum_{j=1}^K(\underline{R}_j + \bar{R}_j)} - \frac{(1 - q_{r,o})\underline{R}\bar{\Omega}_mX_e(n) + q_{r,o}\bar{R}\bar{\Omega}_mX_e(n)}{(\sum_{j=1}^K(\underline{R}_j + \bar{R}_j))^2}
\end{aligned}$$

$$\begin{aligned}
\frac{\underline{R}_{j_w}}{\partial m_{i,j_w}} &= \prod_{i'=1, i' \neq i}^I \underline{Q}_{i',j_w}(m_{i',j_w}) \cdot \frac{1}{n_s} \sum_{r=1}^{n_s} \tilde{\Psi}_r(\underline{\theta}_{i',j_w}^r) \\
\frac{\bar{R}_{j_w}}{\partial m_{i,j_w}} &= \prod_{i'=1, i' \neq i}^I \bar{Q}_{i',j_w}(m_{i',j_w}) \cdot \frac{1}{n_s} \sum_{r=1}^{n_s} \tilde{\Psi}_r(\bar{\theta}_{i',j_w}^r) \\
\frac{\partial \underline{R}_{j_w}}{\partial \theta_{i,j_w}^r} &= \prod_{i'=1, i' \neq i}^I \underline{Q}_{i',j_w}(\theta_{i',j_w}^r) \cdot \frac{1}{n_s} \tilde{\Phi}_r(\theta_{i,j_w}^r) \\
\frac{\partial \bar{R}_{j_w}}{\partial \theta_{i,j_w}^r} &= \prod_{i'=1, i' \neq i}^I \bar{Q}_{i',j_w}(\theta_{i',j_w}^r) \cdot \frac{1}{n_s} \tilde{\Phi}_r(\theta_{i,j_w}^r)
\end{aligned}$$

$$\tilde{\Psi}_r(\theta) = \begin{cases} -\frac{\beta \exp(-\beta(x_{i'} - m_{i',j_w} + |\theta|))}{(1 + \exp(-\beta(x_{i'} - m_{i',j_w} + |\theta|)))^2}, & -\infty < x_{i'} < m_{i',j_w} \\ \frac{\beta \exp(-\beta(x_{i'} - m_{i',j_w} + |\theta|))}{(1 + \exp(-\beta(x_{i'} - m_{i',j_w} + |\theta|)))^2}, & m_{i',j_w} \leq x_{i'} < \infty \end{cases}$$

$$\tilde{\Phi}_r(\theta) = \begin{cases} \frac{\beta \exp(-\beta(x_{i'} - m_{i',j_w} + \theta))}{(1 + \exp(-\beta(x_{i'} - m_{i',j_w} + \theta)))^2}, & -\infty < x_{i'} < m_{i',j_w}, \theta \geq 0 \\ -\frac{\beta \exp(-\beta(x_{i'} - m_{i',j_w} + \theta))}{(1 + \exp(-\beta(x_{i'} - m_{i',j_w} + \theta)))^2}, & m_{i',j_w} \leq x_{i'} < \infty, \theta \geq 0 \\ -\frac{\beta \exp(-\beta(x_{i'} - m_{i',j_w} - \theta))}{(1 + \exp(-\beta(x_{i'} - m_{i',j_w} - \theta)))^2}, & -\infty < x_{i'} < m_{i',j_w}, \theta < 0 \\ \frac{\beta \exp(-\beta(x_{i'} - m_{i',j_w} - \theta))}{(1 + \exp(-\beta(x_{i'} - m_{i',j_w} - \theta)))^2}, & m_{i',j_w} \leq x_{i'} < \infty, \theta < 0 \end{cases}$$

5 Experiments and Data Analysis

In this section, the application of eT2QFNN for RFID localization is discussed. Several experiments are conducted in the real-world environment to evaluate the efficacy of eT2QFNN embracing the MM classifier. The results are compared against

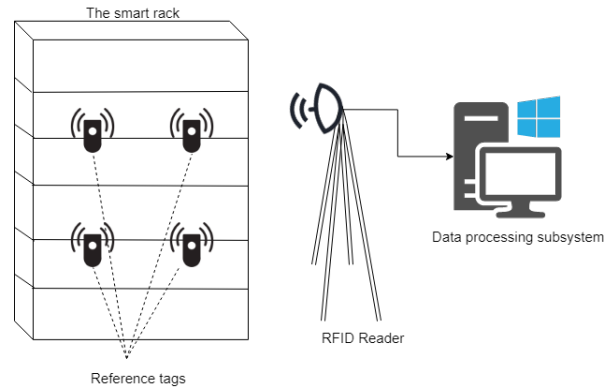


Fig. 5 The illustration of RFID smart rack

4 state-of-the-art algorithm: gClass [Pratama et al, 2014a], pClass [Pratama et al, 2015a], eT2Class [Pratama et al, 2016a] and eT2ELM [Pratama et al, 2015b]. Five performance metrics are used, those are classification rate, the number of fuzzy rule, and the time to execute training and testing processes (execution time). The experiments are conducted under cross-validation and periodic hold-out scenario. The technical details of this experiments are elaborated in the subsection 5.1, while the subsection 5.2 presents the consolidated results.

5.1 Experiment setup

The experiments were conducted at SIMTech laboratory, Singapore. The environment is arranged to resemble the RFID smart rack system. The system utilizes RFID technology to improve the work-flow efficiency by providing the static location of tools and materials for production purposes. As illustrated in the Fig. 5, this system consists of 1 RFID reader, 4 passive RFID tags as references which are fixed in 4 locations, and a data processing subsystem. The dimension of rack is $1510\text{ mm} \times 600\text{ mm} \times 2020\text{ mm}$. The rack has 5 shelves and each shelf can load up to 6 test objects. The number of reference tag indicates that there are 4 class label considered in this experiments. The RFID reader is placed at 1000 mm distance in front of the rack. The antenna is 2200 mm height above the ground. The reader is then connected to an RFID receiver which functions to transmit the signal into a data processing subsystem. Ethernet links is utilized to accommodate the signal transmission. Notably, one may install more reference tags and RFID reader for larger smart rack system to increase the localization accuracy [Chai et al, 2017].

The data processing subsystem has two main components, i.e. data acquisition and the algorithm execution component. The Microsoft Visual C++ based PC application is developed to acquire the RSS information data from all tags, while the

localization algorithm is executed on the MATLAB 2018a online environment. The Reader is configured to report the RSS information every 1 s. The experiment had been conducted for 20 *hours*. There are 283100 observations obtained via the experiment, each reference tag sent up to 70775 observations. It is obvious that these data obtained from the same real-time experiment, and therefore all of them pose the same distribution. Finally, the observation data can be processed to identify the object location by executing the localization algorithm.

5.2 Comparison with existing results

To further investigate the performance of eT2QFNN, it is compared to the existing classification method, i.e. gClass, pClass, eT2Class and eT2ELM. The comparison is conducted in the same computational environments, i.e. MATLAB Online R2018a. The gClass and pClass utilize generalized type-1 fuzzy rule, while the eT2Class and eT2ELM are built upon generalized type-2 fuzzy rule. These methods are able to grow and prune its network structure according to the information provided by the current data stream. All of them except pClass is also capable to merge the similar rules. Further, the eT2ELM is encompassed with active learning and feature selection scenario which helps to discard the unnecessary training data. The eT2QFNN utilizes MM classifier, while others make use MIMO classifier. This classifier is very dependent on rule consequents because it establishes a first-order polynomial for each class. Another characteristic of this classifier is a transformation of true class label to either 0 or 1. As an illustration, if there are 4 class label and the target class is 2, then it will be converted into $[0, 1, 0, 0]$ [Pratama et al, 2015a].

There are two experiments conducted to test the algorithm, i.e. 10-folds cross-validation and direct partition experiments. The first experiment is aimed to test the algorithms consistency while delivering the result. The experiment is started by dividing the data into 10-folds, and 9 folds data is for training, while 1 fold data is for validation. The performance metrics are achieved by averaging the results of 10-folds cross-validation. In the second experiments, the periodic hold-out evaluation scenario is conducted. The algorithms take 50000 data for training and 233100 for validation. The classification rate for the experiments is measured only in the validation phase. In contrast, the execution time is taken into account since the beginning of training phase. In this experiment, we vary $n_s = [0, 10]$ and set $\eta = 0.001$. The results are presented in Table 1 and 2.

It can be seen from the Table 1 that the eT2QFNN delivers most reliable classification rates. Although it employs 4 sub-models to obtain this result which burden the computation, eT2QFNN has the fastest execution time second only to pClass. In terms of network complexity, eT2QFNN generates a comparable number of the fuzzy rule. It worth noting that eT2QFNN is not encompassed with the rule merging and pruning scenario. Further, the number of eT2QFNN rule is less than eT2ELM which has rule pruning and merging scenario. Table 2 confirms the consistency of eT2QFNN while delivering good result. It worth noting that the second experiment

utilizes less data for training, however eT2QFNN maintains the classification rate around 97% which is still comparable to another methods. The execution time is lower than others method except eT2ELM. It is obvious because eT2ELM has the online active scenario which can reduce the training sample.

Table 1 The results of the cross-validation experiment compare to the benchmarked algorithms

Algorithms	Results	
MM-eT2QFNN	Classification rate	0.99 ± 0.05
	Rule	6.23 ± 0.68
	Execution time	618.63 ± 31.64
gClass	Classification rate	0.97 ± 0.006
	Rule	2.4 ± 1.2
	Execution time	1004.36 ± 97.78
pClass	Classification rate	0.97
	Rule	2
	Execution time	369.28 ± 9.99
eT2Class	Classification rate	0.97 ± 0.008
	Rule	2
	Execution time	447.36 ± 11.60
eT2ELM	Classification rate	0.95 ± 0.018
	Rule	37.2 ± 5.95
	Execution time	1324.1 ± 109.47

6 Conclusions

This paper presents an evolving model based on the EIS, namely eT2QFNN. The fuzzification layer relies on IT2QMF, which has a graded membership degree and footprints of uncertainties. The IT2QMF is the extended version of QMF which are able to both capture the input uncertainties and to identify overlaps between input classes. The eT2QFNN works fully in the evolving mode, that is the network parameters and the number of rules are adjusted and generated on the fly. The parameter adjustment scenario is achieved via DEKF. Meanwhile, the rule growing mechanism is conducted by measuring the statistical contribution of the hypothetical rule. The new rule is formed when its statistical contribution is higher than the sum of others multiplied by vigilance parameter. The proposed method is utilized to predict the class label of an object according to the RSS information provided by the reference tags. The conducted experiments simulates the RFID smart rack system which is constructed by 4 reference tags, 1 RFID reader and a data processing subsystem to execute the algorithm. The experiments results show that eT2QFNN is capable of

Table 2 The results of the direct partition experiment compare to the benchmarked algorithms

Algorithms	Results	
MM-eT2QFNN	Classification rate	0.97
	Rule	4.75
	Execution time	131.5
gClass	Classification rate	0.99
	Rule	4
	Execution time	290.83
pClass	Classification rate	0.98
	Rule	2
	Execution time	225.8
eT2Class	Classification rate	0.98
	Rule	2
	Execution time	330.71
eT2ELM	Classification rate	0.98
	Rule	5
	Execution time	41.73

delivering comparable accuracy benchmarked to state-of-the-art algorithms while maintaining low execution time and compact network.

Acknowledgements This project is fully supported by NTU start-up grant and Ministry of Education Tier 1 Research Grant. We also would like to thank Singapore Institute of Manufacturing Technology which provided the RFID data that greatly assisted the research.

References

- Angelov P, Zhou X (2006) Evolving fuzzy systems from data streams in real-time. In: *Evolving Fuzzy Systems, 2006 International Symposium on*, IEEE, pp 29–35
- Bortman M, Aladjem M (2009) A growing and pruning method for radial basis function networks. *IEEE Transactions on Neural Networks* 20(6):1039–1045
- Chai J, Wu C, Zhao C, Chi HL, Wang X, Ling BWK, Teo KL (2017) Reference tag supported rfid tracking using robust support vector regression and kalman filter. *Advanced Engineering Informatics* 32:1–10
- Chen CH, Lin CJ, Lin CT (2008) An efficient quantum neuro-fuzzy classifier based on fuzzy entropy and compensatory operation. *Soft Computing* 12(6):567–583
- Huang GB, Saratchandran P, Sundararajan N (2003) A recursive growing and pruning rbf (gap-rbf) algorithm for function approximations. In: *Control and Automation, 2003. ICCA'03. Proceedings. 4th International Conference on*, IEEE, pp 491–495

- Huang GB, Saratchandran P, Sundararajan N (2004) An efficient sequential learning algorithm for growing and pruning rbf (gap-rbf) networks. *IEEE Transactions on Systems, Man, and Cybernetics, Part B (Cybernetics)* 34(6):2284–2292
- Huang GB, Saratchandran P, Sundararajan N (2005) A generalized growing and pruning rbf (ggap-rbf) neural network for function approximation. *IEEE Transactions on Neural Networks* 16(1):57–67
- Lin CJ, Chen CH (2006) A self-organizing quantum neural fuzzy network and its applications. *Cybernetics and Systems: An International Journal* 37(8):839–859
- Lughofer E, Cernuda C, Kindermann S, Pratama M (2015) Generalized smart evolving fuzzy systems. *Evolving Systems* 6(4):269–292
- Lughofer ED (2008) Flexfis: A robust incremental learning approach for evolving takagi–sugeno fuzzy models. *IEEE Transactions on fuzzy systems* 16(6):1393–1410
- Ni LM, Liu Y, Lau YC, Patil AP (2004) Landmarc: indoor location sensing using active rfid. *Wireless networks* 10(6):701–710
- Ni LM, Zhang D, Souryal MR (2011) Rfid-based localization and tracking technologies. *IEEE Wireless Communications* 18(2)
- Oentaryo RJ, Er MJ, Linn S, Li X (2014) Online probabilistic learning for fuzzy inference system. *Expert Systems with Applications* 41(11):5082–5096
- Pratama M (2017) Panfis++: A generalized approach to evolving learning. arXiv preprint arXiv:170502476
- Pratama M, Anavatti S, Lughofer E, Lim C (2014a) gclass: An incremental meta-cognitive-based scaffolding theory. Submitted to a special issue on *IEEE Computational Intelligence Magazine*
- Pratama M, Anavatti SG, Angelov PP, Lughofer E (2014b) Panfis: A novel incremental learning machine. *IEEE Transactions on Neural Networks and Learning Systems* 25(1):55–68
- Pratama M, Anavatti SG, Joo M, Lughofer ED (2015a) pclass: an effective classifier for streaming examples. *IEEE Transactions on Fuzzy Systems* 23(2):369–386
- Pratama M, Lu J, Zhang G (2015b) A novel meta-cognitive extreme learning machine to learning from data streams. In: *Systems, Man, and Cybernetics (SMC), 2015 IEEE International Conference on, IEEE*, pp 2792–2797
- Pratama M, Lu J, Zhang G (2016a) Evolving type-2 fuzzy classifier. *IEEE Transactions on Fuzzy Systems* 24(3):574–589
- Pratama M, Lughofer E, Er MJ, Rahayu W, Dillon T (2016b) Evolving type-2 recurrent fuzzy neural network. In: *Neural Networks (IJCNN), 2016 International Joint Conference on, IEEE*, pp 1841–1848
- Purushothaman G, Karayiannis NB (1997) Quantum neural networks (qnns): inherently fuzzy feedforward neural networks. *IEEE Transactions on neural networks* 8(3):679–693
- Puskorius GV, Feldkamp LA (1994) Neurocontrol of nonlinear dynamical systems with kalman filter trained recurrent networks. *IEEE Transactions on neural networks* 5(2):279–297

- Soltani MM, Motamedi A, Hammad A (2015) Enhancing cluster-based rfid tag localization using artificial neural networks and virtual reference tags. *Automation in Construction* 54:93–105
- Vuković N, Miljković Z (2013) A growing and pruning sequential learning algorithm of hyper basis function neural network for function approximation. *Neural Networks* 46:210–226
- Yang Z, Zhang P, Chen L (2016) Rfid-enabled indoor positioning method for a real-time manufacturing execution system using os-elm. *Neurocomputing* 174:121–133
- Zhang R, Sundararajan N, Huang GB, Saratchandran P (2004) An efficient sequential rbf network for bio-medical classification problems. In: *Neural Networks, 2004. Proceedings. 2004 IEEE International Joint Conference on, IEEE, vol 3*, pp 2477–2482